Research Article
Viral Hepatitis

JOURNAL
OF HEPATOLOGY

Efficient long-term amplification of hepatitis B virus isolates after infection of slow proliferating HepG2-NTCP cells

Graphical abstract

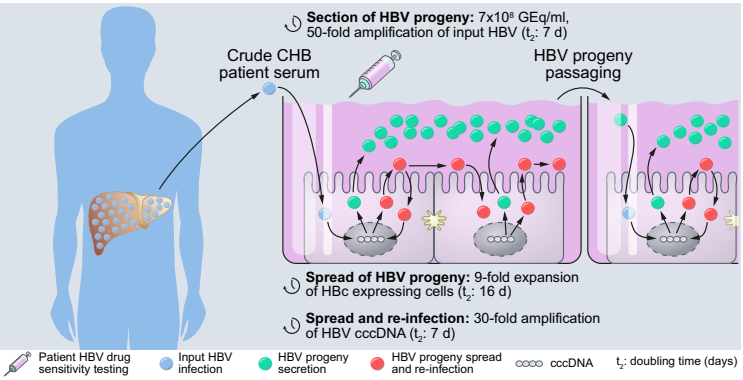

Highlights

- Cell culture system that mimicks complete HBV life cycle from entry to egress.
- Efficient *in vitro* infection with crude HBV patient sera.
- Up to 50- and 1,300-fold net amplification of patient- and cell culture-derived input HBV in the supernatant.
- Polyethylene glycol-independent HBV spread to adjacent cells, forming infected cell clusters.
- Evaluation of patient- and cell culture-derived HBV amplification w/wo antivirals over 8 weeks.

Authors

Alexander König, Jaewon Yang, Eunji Jo, ..., Kwang-Hyub Han, Wolfram Hubert Gerlich, Marc Peter Windisch

Correspondence

marc.windisch@ip-korea.org
(M. Peter Windisch)

Lay summary

Currently available laboratory systems are unable to reproduce the dynamics of hepatitis B virus (HBV) spread through the infected liver and release into the blood. We developed a slowly dividing liver-derived cell line which multiplies infectious viral particles upon inoculation with patient- or cell culture-derived HBV. This new infection model can improve therapy by measuring, in advance, the sensitivity of a patient's HBV strain to specific antiviral drugs.

http://dx.doi.org/10.1016/j.jhep.2019.04.010
 J. Hepatol. 2019, 71, 289–300

Research Article
Viral Hepatitis

JOURNAL OF HEPATOLOGY

Efficient long-term amplification of hepatitis B virus isolates after infection of slow proliferating HepG2-NTCP cells

Alexander König[1,†], Jaewon Yang[1,†], Eunji Jo[1], Kyu Ho Paul Park[1], Hyun Kim[1,2], Thoa Thi Than[1], Xiyong Song[3], Xiaoxuan Qi[3], Xinghong Dai[3], Soonju Park[4], David Shum[4], Wang-Shick Ryu[5], Jung-Hee Kim[6], Seung Kew Yoon[6], Jun Yong Park[7], Sang Hoon Ahn[7], Kwang-Hyub Han[7], Wolfram Hubert Gerlich[8], Marc Peter Windisch[1,2,*]

[1]*Applied Molecular Virology Laboratory, Institut Pasteur Korea, Seongnam-si, South Korea;* [2]*Division of Bio-Medical Science and Technology, University of Science and Technology, 217, Gajeong-ro, Yuseong-gu, Daejeon, South Korea;* [3]*Department of Physiology and Biophysics, School of Medicine, Case Western Reserve University, Cleveland, OH, USA;* [4]*Screening Discovery Platform, Institut Pasteur Korea, Seongnam-si, South Korea;* [5]*Department of Biochemistry, Yonsei University, Seoul, South Korea;* [6]*Catholic University Liver Research Center, The Catholic University of Korea, Seoul, South Korea;* [7]*Department of Internal Medicine, Yonsei University College of Medicine, Seoul, South Korea;* [8]*Institute of Medical Virology, Justus-Liebig-University, Giessen, Germany*

Background & Aims: As hepatitis B virus (HBV) spreads through the infected liver it is simultaneously secreted into the blood. HBV-susceptible *in vitro* infection models do not efficiently amplify viral progeny or support cell-to-cell spread. We sought to establish a cell culture system for the amplification of infectious HBV from clinical specimens.

Methods: An HBV-susceptible sodium-taurocholate cotransporting polypeptide-overexpressing HepG2 cell clone (HepG2-NTCPsec+) producing high titers of infectious progeny was selected. Secreted HBV progeny were characterized by native gel electrophoresis and electron microscopy. Comparative RNA-seq transcriptomics was performed to quantify the expression of host proviral and restriction factors. Viral spread routes were evaluated using HBV entry- or replication inhibitors, visualization of viral cell-to-cell spread in reporter cells, and nearest neighbor infection determination. Amplification kinetics of HBV genotypes B-D were analyzed.

Results: Infected HepG2-NTCPsec+ secreted high levels of large HBV surface protein-enveloped infectious HBV progeny with typical appearance under electron microscopy. RNA-seq transcriptomics revealed that HBV does not induce significant gene expression changes in HepG2-NTCPsec+, however, transcription factors favoring HBV amplification were more strongly expressed than in less permissive HepG2-NTCPsec−. Upon inoculation with HBV-containing patient sera, rates of infected cells increased from 10% initially to 70% by viral spread to adjacent cells, and viral progeny and antigens were efficiently secreted. HepG2-NTCPsec+ supported up to 1,300-fold net amplification of HBV genomes depending on the source of virus. Viral spread and amplification were abolished by entry and replication inhibitors; viral rebound was observed after inhibitor discontinuation.

Conclusions: The novel HepG2-NTCPsec+ cells efficiently support the complete HBV life cycle, long-term viral spread and amplification of HBV derived from patients or cell culture, resembling relevant features of HBV-infected patients.

Lay summary: Currently available laboratory systems are unable to reproduce the dynamics of hepatitis B virus (HBV) spread through the infected liver and release into the blood. We developed a slowly dividing liver-derived cell line which multiplies infectious viral particles upon inoculation with patient- or cell culture-derived HBV. This new infection model can improve therapy by measuring, in advance, the sensitivity of a patient's HBV strain to specific antiviral drugs.

Introduction

Despite vaccination, chronic hepatitis B (CHB) has remained among the most widespread, life-shortening infectious diseases. Two billion people worldwide have been infected with the hepatitis B virus (HBV), including 257 million chronic carriers. Up to 30% of chronically HBV-infected adults will develop liver cirrhosis or hepatocellular carcinoma, accounting for 887,000 deaths annually.[1] Reverse transcriptase inhibitors and interferon-alpha can control viral replication and prevent CHB progression. However, these therapies do not act on HBV genomes in host cell nuclei that persist as covalently closed circular DNA (cccDNA). Thus, current treatment regimens are not curative, requiring lifelong therapy.

HBV has a restricted host range and a narrow tissue tropism which has hampered the study of the HBV life cycle and the discovery of new therapeutic approaches. Only highly differentiated hepatocyte-derived cells from human or tree shrew (Tupaia) can be used for *in vitro* HBV infection studies. Hepatocytes derived from common laboratory animals like mice, rats,

Keywords: Complete HBV life cycle; HepG2-NTCP; Patient-derived HBV; Drug sensitivity; Kinetics of antigen; Virion secretion; cccDNA accumulation; HBV doubling time; HBV spread.
Received 28 September 2018; received in revised form 3 April 2019; accepted 3 April 2019; available online 8 May 2019

* Corresponding author. Address: Applied Molecular Virology Laboratory, Discovery Biology Department, Institut Pasteur Korea, Gyeonggi-do 463-400, South Korea. Tel.: +82-31-8018-8181, fax: +82-31-8018-8014.
E-mail address: marc.windisch@ip-korea.org (M.P. Windisch).
† Alexander König and Jaewon Yang contributed equally to this work.

dogs, macaques or pigs do not support HBV infection.[2,3] The current gold standard for *in vitro* infection studies utilizes primary human hepatocytes (PHHs) and patient-derived HBV. However, PHH drawbacks include high cost, limited availability, difficult handling, donor variability, and dedifferentiation leading to rapid loss of HBV susceptibility and replication.[4] The hepatoma HepaRG cell line requires laborious re-differentiation that results in only moderate HBV susceptibility.[5] Novel models, *i.e.* self-assembling co-cultures (SACC) of PHHs with non-parenchymal liver cells, as well as a 3D microfluidic PHH system, can support persistent infection with cell culture and purified patient-derived HBV strains for 5-6 weeks, but no amplification and spread of HBV has been observed to date, and both models depend on human liver tissue.[6,7] Other promising systems are human hepatocyte-like cells (HLC) generated from induced pluripotent stem cells or embryonic stem cells which are susceptible to HBV and support limited viral production and spread.[8,9]

A major breakthrough was the discovery of the sodium-taurocholate cotransporting polypeptide (NTCP) as the differentiation-dependent, hepatocyte- and species-specific cell membrane HBV receptor.[10] Although hepatoma cell lines, such as HepG2 and Huh-7, replicate HBV after transfection with HBV DNA, they are not susceptible to HBV infection. However, they can be rendered susceptible by NTCP overexpression. Efficient infection of these and other cells requires treatment with polyethylene glycol (PEG) during HBV attachment and/or entry to enhance glycosaminoglycan-dependent binding.[11] Dimethylsulfoxide (DMSO) is used to slow down cell proliferation, extend lifespan, increase differentiation status, and enhance susceptibility and HBV replication. However, following HBV infection and episomal cccDNA formation, these cells fail to amplify the viral genomes, hampering viral progeny production, and spread in cell culture.

HBV-transfected hepatoma cells, including HepAD38 and HepG2.2.15, have been used to produce cell culture-derived HBV (HBVcc) and to investigate late stages of the viral life cycle. Less laborious and expensive *in vitro* infection systems with an unlimited supply that support the complete HBV life cycle and more closely resemble hepatocytes in the human liver, by allowing for more efficient amplification and spread of viral progeny, would be highly desirable (reviewed in 12). In this study, we identify and characterize a slowly proliferating HepG2-NTCP clone that supports the efficient secretion of highly infectious HBV progeny upon infection with patient- and cell culture-derived virus, and elucidate the kinetics and routes of viral amplification during long-term infection.

Materials and methods

HBV infection and progeny passaging

First HBV passage (p1): HepG2-NTCPsec+ were incubated in 384-well plates (8,000 cells/well) for 18 h in infection medium. p1-cells were inoculated at 37 °C for 24 h with HepAD38-cell-harvested HBVcc genotype D (2,500 genome equivalents [GEq]/cell, 5×10^8 GEq/ml) or with diluted crude sera from 7 Korean patients with CHB, unless otherwise indicated, with 4% PEG8000. For inhibition of HBV infection, cells were treated with inhibitors 2 h before and during inoculation. Following inoculum removal and washing, cells were incubated for 120 h in infection medium with or without reference inhibitors. Naïve HepG2-NTCPsec+ p2-cells were seeded in infection medium into 384-well plates 24 h before inoculation. For p2-cell infection, supernatants of HBVcc-infected p1-cells were transferred to p2-cells at 6 days post-infection (dpi) in the presence of 4% PEG. After 24 h, cells were washed and incubated with fresh medium for 120 h.

For further details regarding the materials and methods used, please refer to the CTAT table and supplementary information.

Results

Infectious HBV progeny production in slowly proliferating HepG2-NTCP cells

Our goal was to identify an HBV-susceptible HepG2-NTCP clone with enhanced production of infectious HBV progeny. We subjected a previously described HepG2-NTCP cell clone (parental clone) to reselection for NTCP overexpression by increasing the blasticidin selection pressure (15 μg/ml) for 6 weeks.[13] Five new HepG2-NTCP clones were selected and HBV susceptibility tested (Fig. 1A). The parental cell clone and another published HepG2-NTCP reference clone (sec−), were used as controls.[14] Beside clone #3, all clones showed detectable NTCP expression and similar levels of myrcludex B (MyrB)-sensitive HBV susceptibility (Fig. 1B). To test the production of infectious HBV progeny by the different clones, we infected p1 cells with serially diluted HBV and passaged the supernatants to naïve p2 cells for infection (Fig. 1C). Depending on the inoculum size, p1 infection rates varied between ~10–90% (Fig. 1D, upper panel). Clone #5 was superior in the secretion of infectious viral progeny and was therefore named HepG2-NTCPsec+ (Fig. 1D, lower panel). Only viral progeny secreted from the HepG2-NTCPsec+ infected up to 50% of p2 cells while all other clones showed lower abilities in HBV secretion. Lamivudine (LMV), an HBV replication inhibitor, abrogated the infectivity of the p1 supernatant for p2 cells, demonstrating that the p2 cell infection was caused by secreted progeny virions and not by carryover of input virus (Fig. 1E).

Notably, the NTCP expression level in HepG2-NTCPsec− is 2-fold higher than in sec+ as determined by quantification of immunofluorescence images, leading to increased taurocholic acid uptake and binding capacity for HBV as shown by a 2–10-fold elevated plasma membrane accumulation of myrpreS1-Alexa633 peptide in live-cell imaging and FACS analysis (Fig. S1A-D). Comparing cell doubling times (t_2) identified HepG2-NTCPsec+ with a 2-fold reduced growth rate (t_2 = 13.1 days) relative to that of HepG2-NTCPsec− with a typical t_2 of 6.7 days (Fig. S2A). Slow-growing HepG2-NTCPsec+ were larger and less numerous upon cell confluency (Fig. S2B), with a significantly larger fraction of cells within the non-dividing G0/G1 cell cycle phase (Fig. S2C). DMSO extended the HepG2-NTCPsec+ lifespan, enabling long-term culture for up to 8 weeks without a significant decrease in cell numbers and metabolic activity as shown by robust ATP levels (Fig. S2D). To test whether HBV progeny production in HepG2-NTCP cells depends on the cell cycle, we knocked down CDK6, which regulates the G1/S phase progression (Fig. S2E). After confirming a 70% reduction of *CDK6* mRNA level, HepG2-NTCP cells showed markedly decreased proliferation, a minor increase in the number of *de novo* infected cells, and significantly increased production of infectious HBV progeny (Fig. S2F).

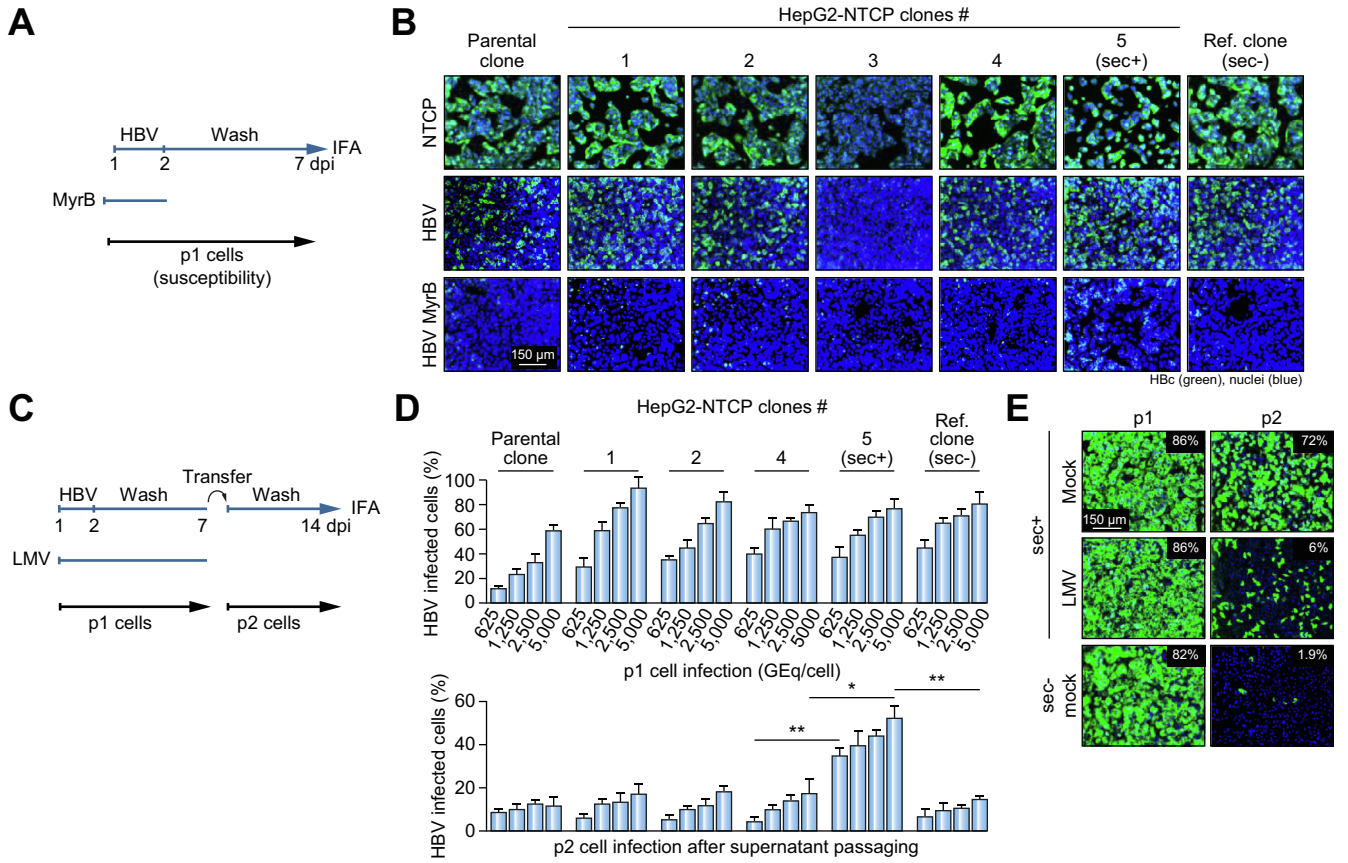

Fig. 1. Selection of a HepG2-NTCP clone capable of secreting infectious progeny HBV. (A) Workflow for HBV infection. Seven different HepG2-NTCP clones were cultured with or w/o MyrB, followed by infection with HBVcc. (B) NTCP-specific immunofluorescence analysis (green, upper panel), HBcAg-specific immunofluorescence analysis (green) of HBV-infected cells w/o (middle panel) or with MyrB treatment (lower panel). Cell nuclei (blue). (C) Workflow of HBV infection and supernatant transfer. Cells (p1) were infected with serially diluted HBVcc and cultured +/- LMV, followed by supernatant transfer to p2 cells. (D) Image quantification of HBV-infected p1 and p2 HepG2-NTCP cells. (E) HBcAg-specific immunofluorescence analysis of p1 and p2 HepG2-NTCPsec− and mock- or 10 µM LMV-treated HepG2-NTCPsec+. Mean HBV infection rates (%) are indicated in each image. Data presented as means ± SD of triplicate wells with 6 images/well (n = 18). Student's *t* test (**p* <0.05, ***p* <0.01, ****p* <0.001, n.s. not significant). HBc, HBV core antigen; HBV, hepatitis B virus; LMV, lamivudine; MyrB, myrcludex B; p1, passage 1; p2, passage 2.

Characterization of HepG2-NTCPsec+ derived HBV progeny

Next, we compared the secretion of HBV over 4 weeks after inoculation of HepG2-NTCPsec− and sec+ with a high-dose of HBVcc (5,000 GEq/cell or 8×10^8 GEq/ml). As a marker of infection, HBV core antigen (HBcAg) was expressed robustly for 4 weeks in > 90% of cells in both clones (Fig. 2A). However, at 4 weeks post infection (wpi), HepG2-NTCPsec− secreted 3-fold lower HBV e antigen (HBeAg) and 16-fold less HBV surface antigen (HBsAg) (Fig. 2B). Also, HBV DNA levels secreted by HepG2-NTCPsec− did not reach the DNA input level whereas HepG2-NTCPsec+ secreted higher numbers of HBV DNA, which demonstrated net amplification of viral genomes (Fig. 2B). We compared secretion of HBV genomes in PHH at 11 and 15 dpi, before the signal vanished at 20 dpi (Fig. S3A). Compared to HepG2-NTCPsec+, we determined a similar daily secretion rate of HBV genomes and HBeAg, but a 4-fold lower production of small HBV surface protein (SHBs) per infected cell by PHH (Fig. S3B). Similar to HepG2-NTCPsec−, parental HepG2-NTCP cells and other clones showed lower secretion levels of all viral markers (Fig. S3C).

The structure of secreted HBV-related particles was analyzed by native western blotting using anti-HBc or anti-preS1 antibodies, which recognize the large HBV surface antigen (LHBsAg). HepG2-NTCPsec− produced low levels of LHBs-enveloped HBcAg capsids (Fig. 2C). In contrast, HepG2-NTCPsec+ secreted increasing high levels of enveloped viral particles (Fig. 2C). Accordingly, infectivity of the supernatants increased over time (Fig. S4). HBV-transfected producer cells HepAD38 secreted 10-fold more non-infectious "naked" capsids than LHBs-enveloped virions (Fig. 2C). Accordingly, HepG2-NTCPsec+ inocula were more infectious than those of HepAD38 cells (Fig. 2E). In contrast to HBV-infected HepG2-NTCPsec− and transfected HepAD38 cells, HepG2-NTCPsec+ secreted >100-fold more LHBs-enveloped HBV particles and no detectable naked capsids. Similarly, the serum from a highly contagious patient with CHB contained high levels of enveloped HBV capsids and no naked capsids (Fig. 2D). The serum also contained slowly migrating and faster-migrating LHBs containing particles without capsids which were absent in the sec+ samples. However, Dane particles of 45 nm in diameter, as well as 23 nm spherical and filamentous subviral particles of heterogeneous length were produced by infected HepG2-NTCPsec+ as visualized by negative-staining electron microscopy (Fig. 2F).

Comparative transcriptomics of HepG2-NTCPsec+ and HepG2-NTCPsec−

In search for cellular factors which could explain the marked differences in HBV progeny secretion between HepG2-NTCPsec

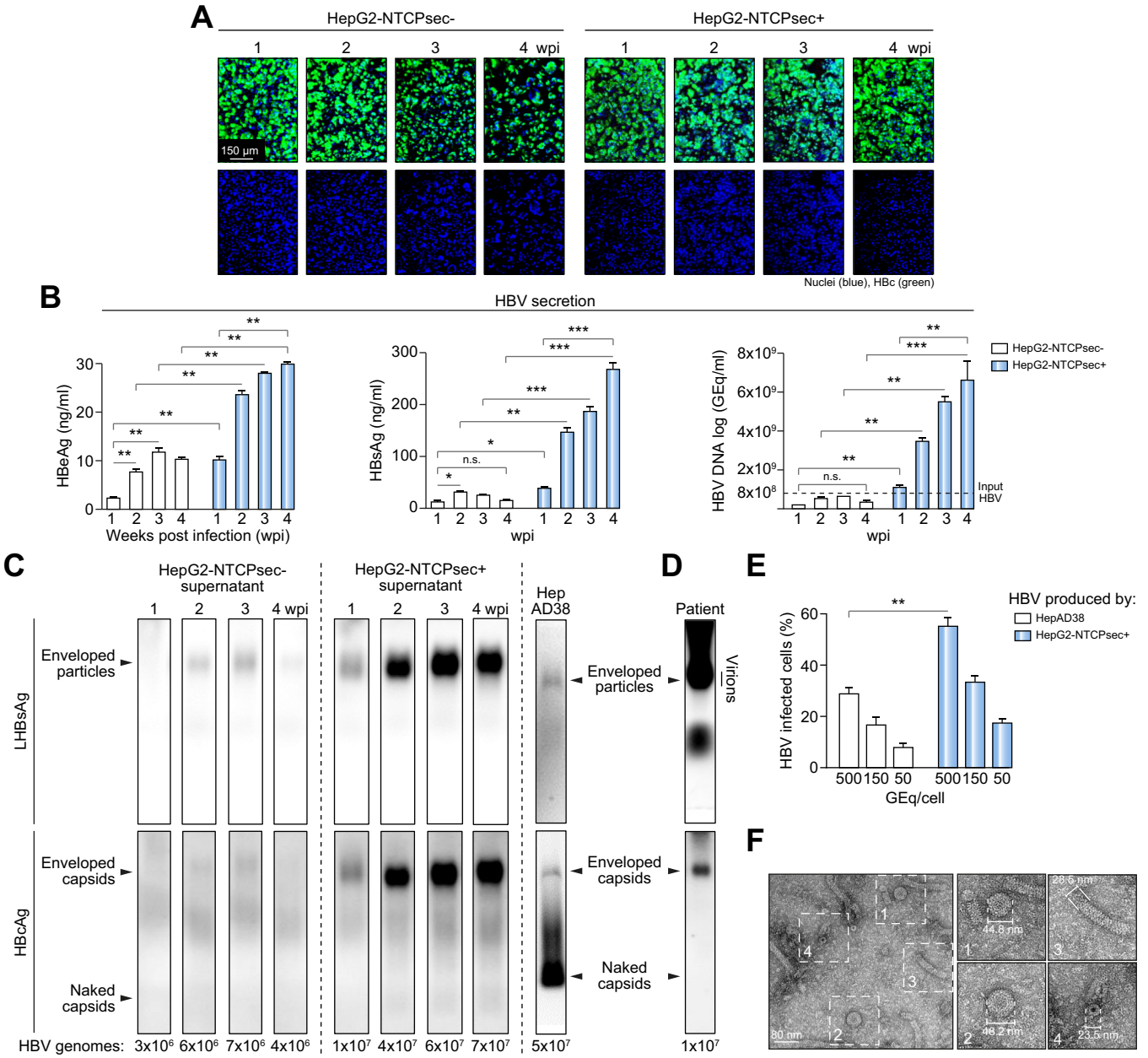

Fig. 2. Infectivity of HepG2-NTCPsec+-released HBV progeny correlates with HBsAg envelopment of nucleocapsids. HepG2-NTCPsec−/sec+ were infected with HepAD38-derived HBV. (A) HBcAg-specific immunofluorescence analysis and nucleus staining of HBV-infected HepG2-NTCPsec−/sec+ from 1-4 wpi. (B) Levels of HBeAg (left), HBsAg (middle) and HBV genomes (right) secreted by HBV-infected HepG2-NTCPsec−/sec+ were analyzed by ELISA or qPCR (input HBV, horizontal line). Supernatants of 20 wells (384-well plate) were pooled and analyzed as duplicates. (C) LHBs of enveloped HBV particles and HBcAg of enveloped capsids (virions) and non-enveloped naked capsids were analyzed by native western blotting. HBV genome numbers per 10 µl of supernatants are indicated. (D) HBV particle pattern in serum of a patient with CHB. (E) Percent infected HepG2-NTCPsec+ (7 dpi) inoculated with HepAD38- or HepG2-NTCPsec +-derived HBV. (F) Negative-staining electron microscopy of HBV particles produced by infected HepG2-NTCPsec+. (*p <0.05, **p <0.01, ***p <0.001, n.s. not significant). HBcAg, HBV core antigen; HBeAg, HBV e antigen; HBV, hepatitis B virus; LHBs, large HBV surface protein; qPCR, quantitative PCR; HBsAg, HBV surface antigen.LHB.

+ and sec−, we conducted a comparative transcriptomic analysis in the presence and absence of HBV (Fig. 3A). Strikingly, using stringent parameters of p value <0.01 and q-value <0.05 for the analysis of triplicates, no gene transcripts were uniformly induced or repressed by HBV infection of HepG2-NTCPsec+ compared to naïve sec+, just as shown for chimpanzees during the lag phase of HBV infection (weeks 0–2) or the phase of logarithmic expansion (weeks 4–6) (Fig. 3A, left).[15] However, in HepG2-NTCPsec− that fail to produce infectious progeny virions, 1,364 genes were changed due to HBV infection (689 upregulated, 675 downregulated) (Fig. 3A, right). Comparing the total transcriptome comprising 18,149 genes, 5,494 genes were significantly differentially expressed between HBV-infected HepG2-NTCPsec+ and sec− (2,755 upregulated and 2,793 downregulated in sec+) (Fig. 3B) including host factors related to HBV entry, transcription, assembly and release.

As already demonstrated at the protein level (Fig. S1), *NTCP (SLC10A1)* RNA levels were ~2-fold higher in HepG2-NTCPsec− (Fig. 3C). Furthermore, most genes related to HBV attachment, *e.g.* heparan sulfate proteoglycan (HSPG), AGRN,

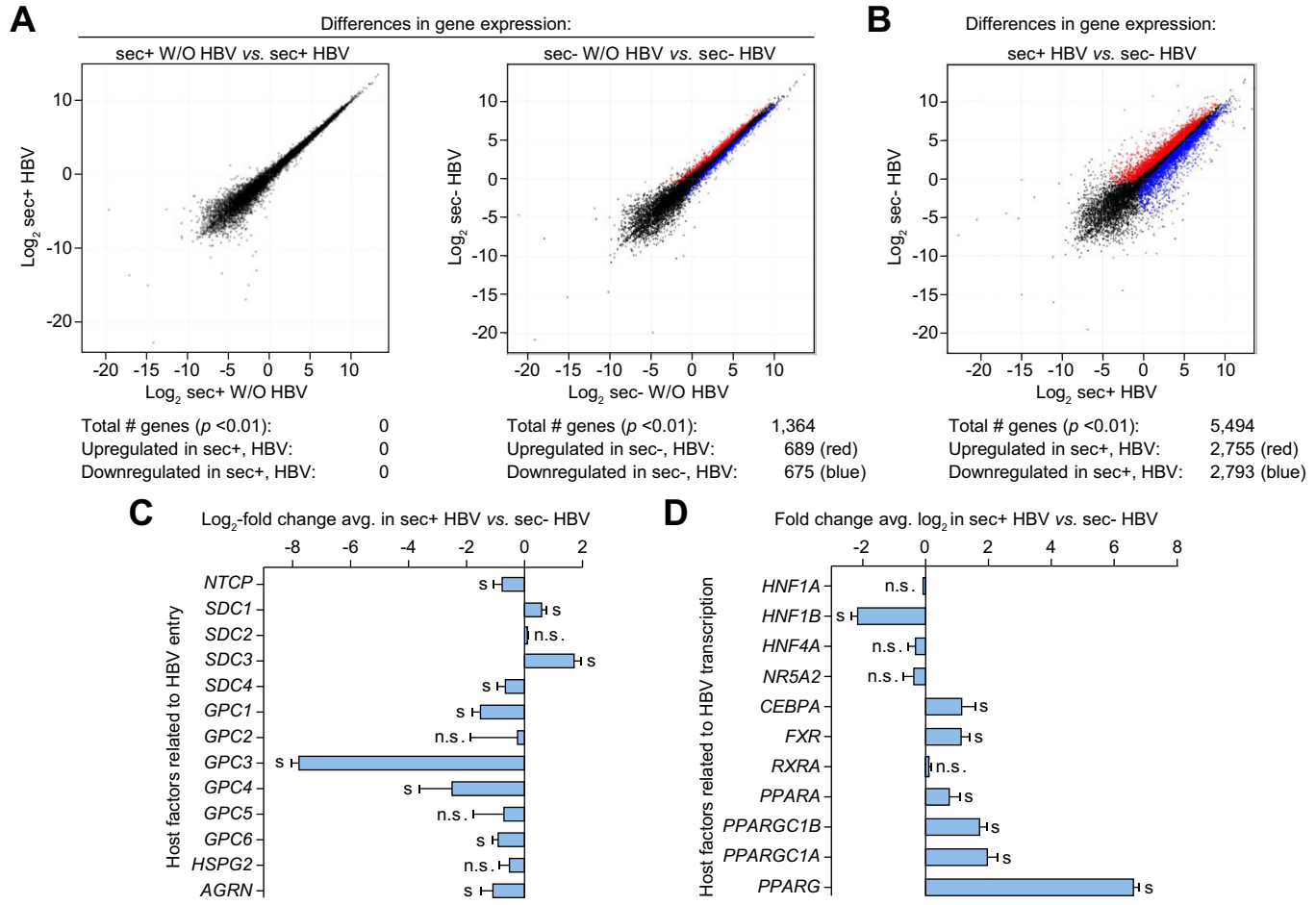

Fig. 3. Comparative transcriptomic analysis of HepG2-NTCPsec+ and sec− in the presence or absence of HBV. Total RNA was isolated at 2 weeks from naïve or HBV-infected HepG2-NTCPsec+/sec−. A cDNA library was generated and sequenced for mRNA comprising a total of 18,149 genes. (A) Scatter plots of differentially expressed genes in HepG2-NTCPsec+ w/o HBV *vs.* sec+ with HBV (left) or HepG2-NTCPsec− w/o HBV *vs.* sec− with HBV (right). (B) Scatter plots of differentially expressed genes in HepG2-NTCPsec+ with HBV *vs.* HepG2-NTCPsec− with HBV. (C-D) Log_2-fold change in gene expression related to HBV entry (C) or transcription (D) in HepG2-NTCPsec+ with HBV *vs.* HepG2-NTCPsec− with HBV. Statistical significance was determined for the analysis of triplicates (s, p <0.01 and q <0.05; n.s., not significant). HBV, hepatitis B virus.

glypicans (GPC) and syndecan 4 (SDC) were more highly expressed in HepG2-NTCPsec− (Fig. 3C). Among 11 previously described HBV transcription factors, *CEBPA, FXR, PPARA, PPARGC1A/B* and *PPARG* were 2- to 100-fold upregulated while only *HNF1B* was 5-fold downregulated in sec+ compared to sec− using stringent parameters of p value <0.01 and q-value <0.05 for the analysis of triplicates (Fig. 3D). Furthermore, *DDX3X* and *DDX3Y*, 2 cellular RNA helicases with known inhibitory effects on HBV replication, were 6- and 2-fold higher expressed in HepG2-NTCPsec−, respectively (Fig. S5). However, HBV restriction host factor *APOBEC3G* was 4-fold higher expressed in sec+. Genes related to the preS1-dependent virion envelopment as well as ESCRT0 complex were mainly upregulated in sec+, while the ESCRT I, II, III secretory complexes which are hijacked by HBV for egress, show a more heterogeneous expression pattern (Fig. S5).

Secretion of infectious progeny drives spread, re-infection, cccDNA replenishment, and HBV amplification in HepG2-NTCPsec+

Considering the high susceptibility and efficient infectious progeny secretion from HepG2-NTCPsec+, we followed HBV spread in long-term (6-week) cultures (Fig. 4A). Inoculation with 500 GEq/cell resulted in an initial infection rate of ~30% at 1 wpi, followed by a steady increase, plateauing at 80% by 4–5 wpi (Fig. 4B). LMV suppressed this increase, indicating the spread of newly produced viral progeny and ruling out delayed *de novo* infection by residual input HBV. Viral spread was abrogated by neutralizing anti-HBs antibodies, indicating that HBV spreads via the release of enveloped viral progeny into the extracellular space. Moreover, HBV spread was also efficiently inhibited in the presence of heparin, MyrB, or anti-preS1 antibodies in a dose-dependent manner (Fig. 4C), indicating that like HBV entry during inoculation with exogenous virus, the HBV S- and preS1 domain as well as cellular HSPG and NTCP are crucial entry factors for spread.

HBV spread correlated with accumulation of intracellular cccDNA (Fig. 4D). As cccDNA is the template for pregenomic RNA (pgRNA) which is converted into the relaxed circular DNA (rcDNA) present in mature nucleocapsids and infectious HBV, intracellular rcDNA synthesis also increased over time (Fig. 4D). New cccDNA is, in turn, generated from rcDNA reimported into the nucleus via recycling of *de novo* synthesized cytoplasmic nucleocapsids or via receptor-mediated entry of released virions. LMV, which blocks reverse transcription of pgRNA into rcDNA, prevented cccDNA replenishment via both

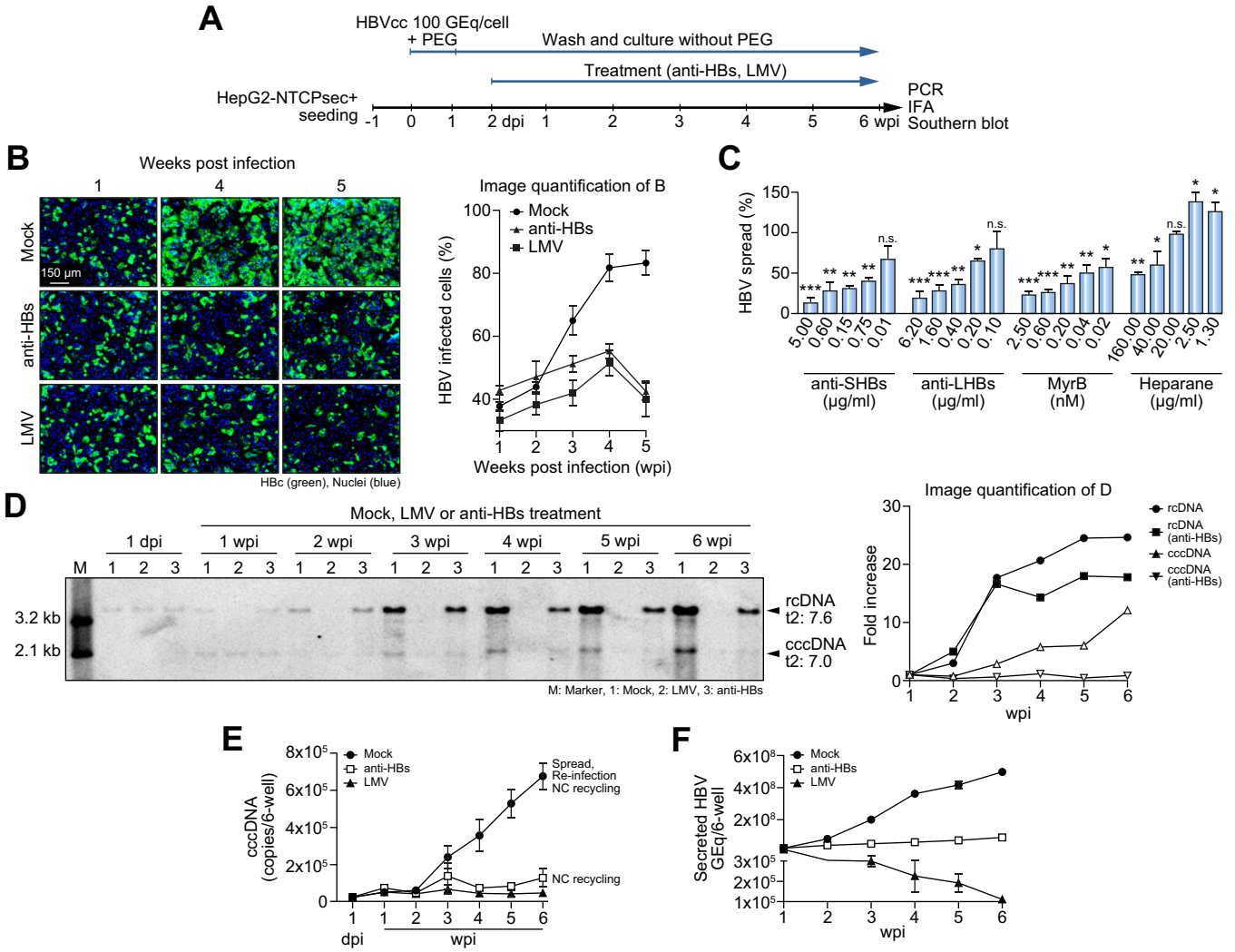

Fig. 4. The cccDNA pool in HepG2-NTCPsec+ cells is predominantly replenished via an extracellular route of spread and re-infection. (A) HepG2-NTCPsec+ were infected with HBVcc. The cells were subjected to mock, LMV, or anti-HBs, anti-LHBs, heparan, MyrB treatments for 6 weeks. (B) HBV-infected cells were visualized by immunofluorescence analysis of HBcAg. (C) Dose-dependent inhibition of HBV spread by entry inhibitors anti-SHBs, anti-preS1 LHBs directed antibodies (MA18/07), MyrB and heparan. (D) Southern blot of HBV cccDNA and rcDNA, and semiquantitative analysis of respective bands. (E) Quantification of cccDNA by qPCR. (F) Quantification of secreted rcDNA genomes by qPCR. Data presented as means ± SD of duplicate or triplicate wells. (*p <0.05, **p <0.01, ***p <0.001, n.s. not significant). cccDNA, covalently closed circular DNA; HBV, hepatitis B virus; HBVcc, cell culture derived HBV; LHBs, large HBV surface protein; LMV, lamivudine; MyrB, myrcludex B; qPCR, quantitative PCR; SHBs, small HBV surface protein.

pathways (Fig. 4D). Anti-HBs treatment reduced, rather than abrogated, rcDNA synthesis by preventing viral spread. However, in quantitative PCR (qPCR) we confirmed that entry inhibitors suppressed cccDNA formation, suggesting that new cccDNA is predominantly derived from *de novo* infection, rather than from recycling of intracellular nucleocapsids (Fig. 4E). We estimated that entry-dependent, extracellular routes account for 88% of HBV genome amplification, with intracellular pathways accounting for no more than 12% of cccDNA replenishment. Secretion of viral genomes similarly increased over time, a trend blocked by anti-HBs and LMV (Fig. 4F). Total rebound of HBV progeny secretion occurred 1–2 weeks after LMV withdrawal (Fig. S4).

At later time points, when *de novo* infection by spread to naïve cells became undetectable, cccDNA and secreted viral genomes continued accumulating, which was prevented by entry and replication inhibitors. Using values of total cell number, the percentage of infected cells and the total number of cccDNA molecules obtained from qPCR (Fig. 4E), we calculated that the number of cccDNA molecules per infected cell was increasing constantly from ~1–8 within 6 weeks. In line with this, inoculation of sec+ with a high virus load and maintaining the cells with a constantly high infection rate of 80–90% over 8 weeks (Fig. S6A) showed a weekly increase of secreted HBV DNA, HBsAg and HBeAg levels over the entire assay period (Fig. S6B). The increase was blocked by replication or entry inhibitors when added to the cells at 2 dpi, indicating that re-infection of already infected cells substantially contributes to HBV amplification. Long-term treatment with the inhibitors had no significant impact on cell viability (Fig. S6C).

HBV progeny spreads preferably to adjacent cells

The spatio-temporal pattern of HBV spread in infected cell cultures (Fig. 5A) was followed by whole-well imaging of HBcAg-positive cells using dedicated image mining software (Fig. S7A). Evaluation of distance between infected cells

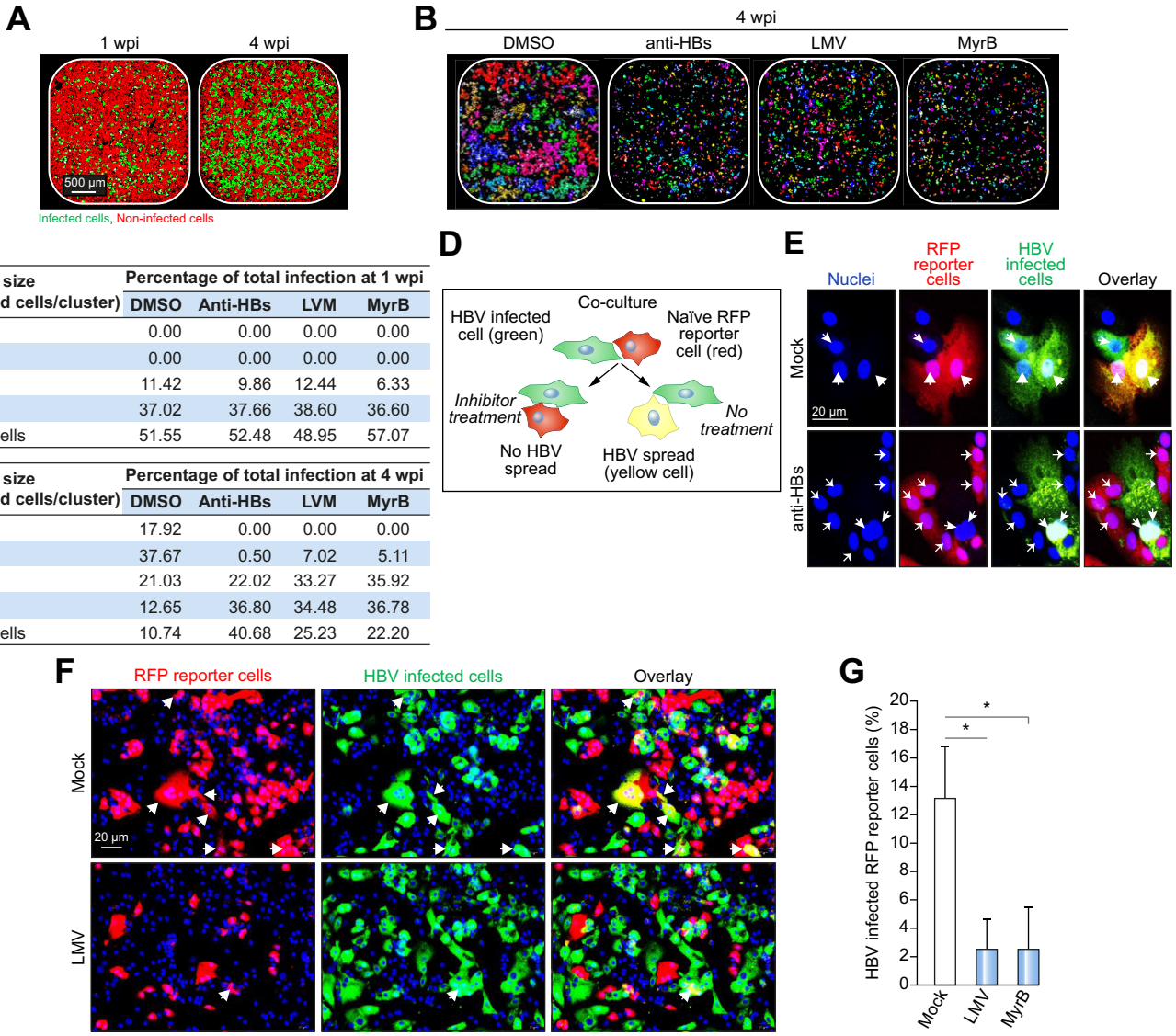

Cluster size (infected cells/cluster)	Percentage of total infection at 1 wpi			
	DMSO	Anti-HBs	LVM	MyrB
>50	0.00	0.00	0.00	0.00
11-50	0.00	0.00	0.00	0.00
4-10	11.42	9.86	12.44	6.33
2-3	37.02	37.66	38.60	36.60
Single cells	51.55	52.48	48.95	57.07

Cluster size (infected cells/cluster)	Percentage of total infection at 4 wpi			
	DMSO	Anti-HBs	LVM	MyrB
>50	17.92	0.00	0.00	0.00
11-50	37.67	0.50	7.02	5.11
4-10	21.03	22.02	33.27	35.92
2-3	12.65	36.80	34.48	36.78
Single cells	10.74	40.68	25.23	22.20

Fig. 5. HBV spreads to adjacent HepG2-NTCPsec+ cells. (A) Full-well images of HBVcc-infected (green) and uninfected (red) cells at 1 and 4 wpi. (B) Cell-to-cell distance analysis grouped HBV-infected cells into clusters highlighted using pseudo-colors. (C) Size categorization of HBV-positive clusters. Relative quantification of infected cells belonging to different cluster sizes at 1 and 4 wpi. (D) Co-culture of infected unlabeled and naïve RFP reporter HepG2-NTCPsec+. (E-F) Representative high magnification images of HBVcc-infected HepG2-NTCPsec+ (green, open arrowheads), infected RFP reporter (yellow overlay, closed arrowheads), and uninfected RFP reporter cells (red, stealth-shaped arrowheads) +/- anti-HBs (E) and overview images under Mock and LMV conditions (F). (G) Quantification of HBV-infected reporter cells. Mean and SD values were calculated from 10 images. Data presented as means ± SD of triplicate wells. (*p <0.05, **p <0.01, ***p <0.001, n.s. not significant). HBs, HBV surface protein; HBV, hepatitis B virus; HBVcc, cell culture-derived HBV; LMV, lamivudine; MyrB, myrcludex B; RFP, red fluorescent protein; wpi, weeks post infection.

revealed the formation of HBV-positive cell clusters (Fig. S7B). The HBV-infected clusters expanded over time, while entry inhibitors MyrB and anti-HBs prevented the formation of larger clusters (Fig. 5B). Mock-treated infected single cells rapidly expanded to >50% of infected cells within clusters of >10 infected cells/cluster at 4 wpi, whereas inhibitor treatment significantly reduced the formation of larger cluster sizes (Fig. 5C).

To further visualize HBV spread on a single-cell level, infected HepG2-NTCPsec+ were co-cultured for 1 week with naïve HepG2-NTCPsec+ expressing the red fluorescent protein (Fig. 5D). Infected reporter cells were predominantly observed adjacent to *de novo* HBV-infected cells, indicating that virus transmission followed a cell-to-cell route (Fig. 5E). MyrB and LMV reduced HBV spread to reporter cells by ~6-fold (Fig. 5F-G).

HBV in sera of patients with CHB persistently amplifies and spreads in HepG2-NTCPsec+

As HepG2-NTCPsec+ supported propagation of HBVcc, we further tested whether these cells support the propagation of patient-derived HBV (HBVpt). We inoculated sec+ with 0.1–20 µl of crude patient sera from 7 Korean patients with CHB and differences in viral load and HBeAg status (Fig. 6A). As determined by immunofluorescence of HBc expression (Fig. 6B), at 1 wpi, 4 out of 7 sera were found to be clearly infectious with >2× the cut-off of 1% infected cells and infection rates proportional to the inoculum concentration in GEq/cell (Fig. 6C). Serum from patient #1 and #2, bearing the highest viral loads, resulted in 47% and 56% infected cells within 1 week, respectively, when inoculated with 5 µl serum, equivalent to 3,400 and 900 GEq/cell (Fig. 6C). Sporadic, single infected cells were

A

Source		Patient 1	Patient 2	Patient 3	Patient 4	Patient 5	Patient 6	Patient 7
Genotype		C1	C	C	C	C1	C	C
Serum	GEq/ml	5.45E + 09	1.45E + 09	4.07E + 08	1.05E + 07	1.83E + 06	2.14E + 07	3.46E + 08
	HBs ng/ml	1.30E + 05	2.30E + 05	1.53E + 04	3.27E + 03	3.94E + 03	5.02E + 03	4.13E + 04
	Ratio GEq/HBs	4.19E + 04	6.30E + 03	2.66E + 04	3.21E + 03	4.64E + 02	4.26E + 03	8.38E + 03
	HBe	+	+	+	-	+	-	-

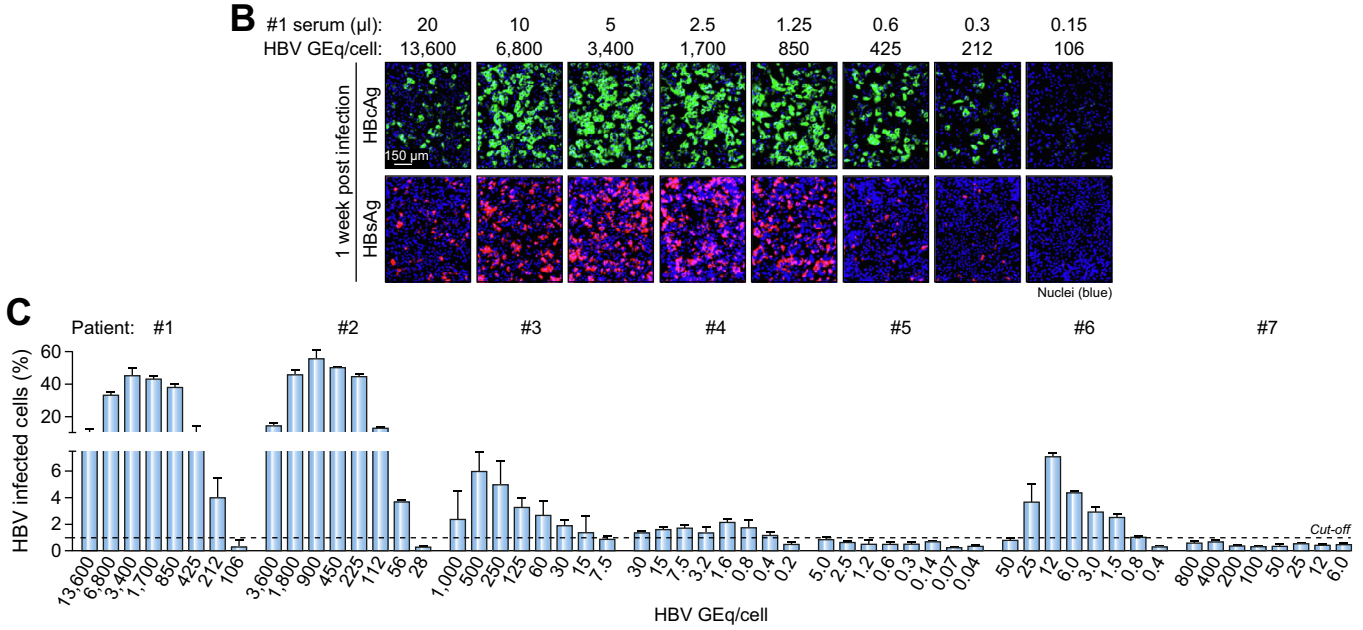

Fig. 6. Susceptibility of HepG2-NTCPsec+ to HBV genotype C clinical samples. (A) Sequencing confirmed genotype, viral genome and HBsAg load, ratio of viral genomes per ng HBs and HBeAg status of 7 patient sera. (B) Cells were inoculated with serial dilutions of crude sera from 7 patients with CHB. Representatively, patient #1 infection visualized at 7 dpi by immunofluorescence analysis of HBcAg and HBsAg. (C) HBcAg-positive cells were quantified for infections with 7 patient sera at 1 wpi. Data presented as means ± SD of triplicate wells with 6 images/well (n = 18). CHB, chronic HBV infection; dpi, days post infection; HBcAg, HBV core antigen; HBeAg, HBV e antigen; HBsAg, HBV surface antigen; HBV, hepatitis B virus; wpi, weeks post infection.

detected using a minimum of 2 GEq/cell of HBVpt #6. The negative results for patients #4 and #5, the positive result of patient #6 and the endpoint dilution enables the definition of a minimum infectious dose, suggesting that the detection limit for infectious virions in serum at 1 wpi is 2×10^7 to 3×10^8 GEq/ml. However, serum of patient #7 caused no detectable infection within 1 week despite a relatively high viral load of 4×10^8 GEq/ml (up to 800 GEq/cell).

Expanding the assay duration, we detected delayed infection for the initially negative sera #4, #5, #7 with 2, 16 and 5% HBV-positive cells at 8 wpi (Table 1). We monitored secreted viral structural antigens, and viral genomes over 8 weeks via ELISA and qPCR. Due to the high input virus inoculum, HBV genomes and HBsAg decreased during the first weeks, before viral markers increased at later assay time points in most cases of HBVpt infections. The earliest time point of inflection of viral genomes was determined at 1 wpi for patient #2 and at 3 wpi for patients #3, #5, and #6. Due to the relatively lower sensitivity of ELISA, HBsAg inflection was detectable 1–3 weeks later. The weekly increasing secretion rate reached between 6×10^3–5×10^8 GEq/ml and <0.1 to up to 316 ng/ml HBsAg at 7 or 8 wpi, paralleled by the expansion of HBV-infected cells by viral spread. Differences in the secretion capacity correlated clearly with the range of infection rates between 3–78%. For HBVcc genotype D and B, the time point of inflection was reached at 1 and 3 wpi, respectively. Taken together, the larger inocula of HBVpt genotype C infected cells and replicated as efficiently as HBVcc with genotype D or B. On average, for genotypes D, C and B, 7×10^7, 3.6×10^5 and 6.5×10^6 HBV genomes per ng of SHBs were secreted weekly during the last 3 weeks, respectively, indicating a 200- and 10-fold higher ratio of secreted genomes per SHBs for genotype D HBVcc.

To evaluate the HBV patient strain-specific antiviral treatment sensitivity, HepG2-NTPCsec+ were inoculated with 0.6 µl (400 GEq/cell, 3×10^7 GEq/ml) serum of patient #1, the 2-fold minimal infectious dose (Fig. 7A), resulting in a low initial infection rate. Until 3 wpi, only minor secretion of HBVpt genomes and clearance of input HBsAg were observed (Fig. 7B). At 4 wpi, HBVpt genome and HBsAg secretion increased significantly with a 50-fold net amplification of accumulated secreted viral genomes until 8 wpi relative to input (1.6×10^9 GEq/ml). HBcAg staining revealed that amplification of secreted viral markers was paralleled by *de novo* infection of naïve cells increasing from 9% up to 70% within 8 weeks (Fig. 7C). Anti-HBs antibody, anti-preS1 antibody MA18/7 (data not shown), and MyrB blocked both amplification of secreted viral markers and *de novo* infection by HBV progeny (Fig. 7B-C). Inhibition by LMV underscored that newly produced viral progeny caused the increase in *de novo* infected cells. During the ramp-up phase of the viral spread between 3–7 wpi, secreted HBV genomes amplified with a markedly shorter t_2 (5.9 days) relative to t_2 in *de novo* infected cells (14.2 days). Consequently, the number

Table 1. Genotype-specific amplification and spread kinetics of patient- and cell culture-derived HBV in HepG2-NTCPsec+. HepG2-NTCPsec+ were inoculated with 5 µl serum of 7 different patients with genotype C CHB, bearing different viral loads or with cell culture-derived genotype D or B HBV and cultured for 8 weeks. The ratio of infected cells and secreted viral markers were monitored. Data presented as means of 1 experiment. Supernatants of 12 wells/data-point (384-well plate) were pooled and analyzed in duplicates.

Source			Patient 1	Patient 2	Patient 3	Patient 4	Patient 5	Patient 6	Patient 7	Cell culture	
Genotype			C1	C	C	C	C1	C	C	D	B
Inoculum		GEq/ml	5.45E+08	1.45E+08	4.07E+07	1.05E+06	1.83E+05	2.14E+06	3.46E+07	1.00E+07	1.49E+08
		HBs ng/ml	1.30E+04	2.30E+04	1.53E+03	3.27E+02	3.94E+02	5.02E+02	4.13E+03	0.81	8.93
		Ratio GEq/HBs	4.19E+04	6.30E+03	2.66E+04	3.21E+03	4.64E+02	4.26E+03	8.38E+03	1.23E+07	8.39E+04
Weeks post infection	1	% infected cells	33	12	5	0.2	0.3	3	0.4	9	9
		GEq/ml	2.10E+07 *	3.30E+07	2.10E+06	3.30E+05	7.00E+03	6.00E+05	7.90E+06	6.00E+07 *	7.30E+07
		HBs ng/ml	6.50E+02	6.32E+02	5.3E+02	1.86E+02	6.20E+01	6.42E+02	1.91E+02	4.00	9.00
		Ratio GEq/HBs	3.23E+04	5.22E+04	3.96E+03	1.77E+03	1.13E+02	9.35E+02	4.14E+04	1.50E+07	8.11E+06
	2	% infected cells	62	45	14	0.7	0.9	12	2	10	27
		GEq/ml	4.00E+07	2.00E+07	1.10E+05	1.60E+05	4.30E+03	3.90E+05	3.40E+05	1.00E+08	2.40E+07
		HBs ng/ml	3.03E+02	4.84E+02	1.22E+02	5.1E+01	1.80E+01	1.60E+02	2.20E+01	4.00	1.00E+01
		Ratio GEq/HBs	1.32E+05	4.13E+04	9.02E+02	3.14E+03	2.39E+02	2.44E+03	1.55E+04	2.50E+07	2.40E+06
	3	% infected cells	74	52	19	1.5	4	15	3	12	30
		GEq/ml	4.90E+07	8.00E+06	4.30E+04 *	1.70E+04	1.90E+03 *	2.30E+05 *	1.70E+04	2.00E+08	1.60E+07
		HBs ng/ml	1.63E+02	3.19E+02	2.3E+01	7.00	3.00	2.80E+01	1.00	4.00	8.00 *
		Ratio GEq/HBs	3.01E+05	2.51E+04	1.87E+03	2.43E+03	6.33E+02	8.21E+03	1.70E+04	5.00E+07	2.00E+06
	4	% infected cells	73	60	19	0.8	2	15	2	18	32
		GEq/ml	6.90E+07	5.00E+06 *	4.40E+04	2.90E+03	4.80E+03	3.80E+05	2.60E+03 *	5.00E+08	1.00E+07 *
		HBs ng/ml	1.43E+02 *	8.00E+01 *	6.00	2.00	1.00	1.10E+01 *	<0.10	4.00 *	9.00
		Ratio GEq/HBs	4.83E+05	6.25E+04	7.33E+03	1.45E+03	4.80E+03	3.45E+04	>2.60E+04	1.25E+08	1.11E+06
	5	% infected cells	75	60	22	0.9	6	26	3	32	46
		GEq/ml	1.90E+08	1.20E+07	1.30E+05	1.40E+03 *	2.00E+04	1.20E+06	2.90E+03	1.00E+09	7.80E+07
		HBs ng/ml	2.50E+02	1.13E+02	2.00 *	1.00	1.00 *	2.80E+01	<0.10	1.20E+01	2.50E+01
		Ratio GEq/HBs	7.60E+05	1.06E+05	6.50E+04	1.40E+03	2.00E+04	4.29E+04	>2.90E+04	8.33E+07	3.12E+06
	6	% infected cells	68	67	31	5.3	12	41	7	51	51
		GEq/ml	4.30E+08	3.80E+07	4.60E+05	3.90E+03	9.60E+04	6.60E+06	3.80E+03	2.00E+09	2.00E+08
		HBs ng/ml	2.72E+02	1.38E+02	1.10E+01	<0.10	2.00	6.00E+01	<0.10	2.90E+01	3.10E+01
		Ratio GEq/HBs	1.58E+06	2.75E+05	4.18E+04	>3.90E+04	4.80E+04	1.10E+05	>3.80E+04	6.90E+07	6.45E+06
	7	% infected cells	78	72	42	2.6	7	50	3	67	65
		GEq/ml	4.50E+08	4.60E+07	1.40E+06	1.30E+04	5.70E+05	1.90E+07	5.50E+03	3.00E+09	3.50E+08
		HBs ng/ml	3.16E+02	1.58E+02	1.60E+01	<0.10	3.00	9.30E+01	<0.10	4.60E+01	4.50E+01
		Ratio GEq/HBs	1.42E+06	2.91E+05	8.75E+04	>1.30E+05	1.90E+05	2.04E+05	>5.50E+04	6.52E+07	7.78E+06
	8	% infected cells	75	71	47	2	16	59	5	67	69
		GEq/ml	5.30E+08	8.90E+07	2.60E+06	8.90E+03	1.90E+05	4.40E+07	6.20E+03	7.00E+09	4.30E+08
		HBs ng/ml	3.09E+02	1.68E+02	2.50E+01	<0.10	4.00	1.96E+02	<0.10	1.04E+02	4.90E+01
		Ratio GEq/HBs	1.72E+06	5.30E+05	1.04E+05	>8.9E+04	4.75E+04	2.24E+05	>6.20E+04	6.73E+07	8.78E+06

CHB, chronic HBV infection; GEq, genome equivalents; HBs, HBV surface protein; HBV, hepatitis B virus.
* Time point of inflection.

of secreted HBV genomes per infected cell per day increased nearly 5-fold between 3 and 8 wpi (Fig. 7D).

Side-by-side, we infected with genotype D HBVcc using 60 GEq/cell (0.01 µl, 1×10^7 GEq/ml) for inoculation (Fig. S8). At 1 wpi, HBVcc genome and HBsAg secretion increased significantly with a 1,300-fold net amplification of accumulated viral genomes relative to input until 8 wpi (1.3×10^{10} GEq/ml) (Fig. S8A). Calculated t_2, as well as the antiviral effect via inhibitor treatment were comparable between the 2 different virus sources and genotypes. Furthermore, a partial viral rebound after MyrB and LMV discontinuation during the last 4 weeks were observed for both viruses. However, a partial rebound after anti-HBs withdrawal was only detectable in genotype D HBVcc-infected cells (Fig. S8A-C).

Discussion

Many viruses can be directly isolated from patients for propagation and passaging in cell culture and amplification of viral progeny. Such *in vitro* approaches allow for the selective isolation of infectious strains within the viral quasispecies pool and the analysis of strain-specific features, like replication efficiency and treatment sensitivity. Up to date, humanized mice are used for efficient amplification of infectious patient- or cell culture-derived HBV (reviewed in 12). Cell culture systems for *in vitro* HBV infection do not support the efficient secretion and amplification of progeny virus. PHHs are capable of secreting HBV efficiently with published values of up to 150 IU/ml SHBs and 2×10^7 GEq/ml (Table S1), but are too fragile in handling, limited in susceptibility and expensive. For HepaRG as well as HepG2-NTCP cells, lower values of 16 and 14 IU/ml SHBs and $\sim 1 \times 10^6$ GEq/ml are reported. The maximum weekly secretion capacity of HepG2-NTCPsec+ reaches 253 IU/ml SHBs and up to 1×10^{10} GEq/ml, 2–20-fold and 500–10,000-fold more SHBs and HBV genomes compared to published values of PHH, HepaRG and other HepG2-NTCP cells infected with HBVcc genotype D.

To our knowledge, we developed the first continuous cell line capable of 1-step net amplification of infectious HBV. Decelerated cell proliferation, extended lifespan, increased G1/S cell ratio, balanced expression of NTCP and HSPG, high expression of HBV-related transcription factors and low expression of HBV restrictive factor DDX3 contribute to increased production of infectious HBV progeny in HepG2-NTCPsec+. Our results confirm previous reports showing that cellular factors restricting HBV replication are linked to the differentiation status of hepa-

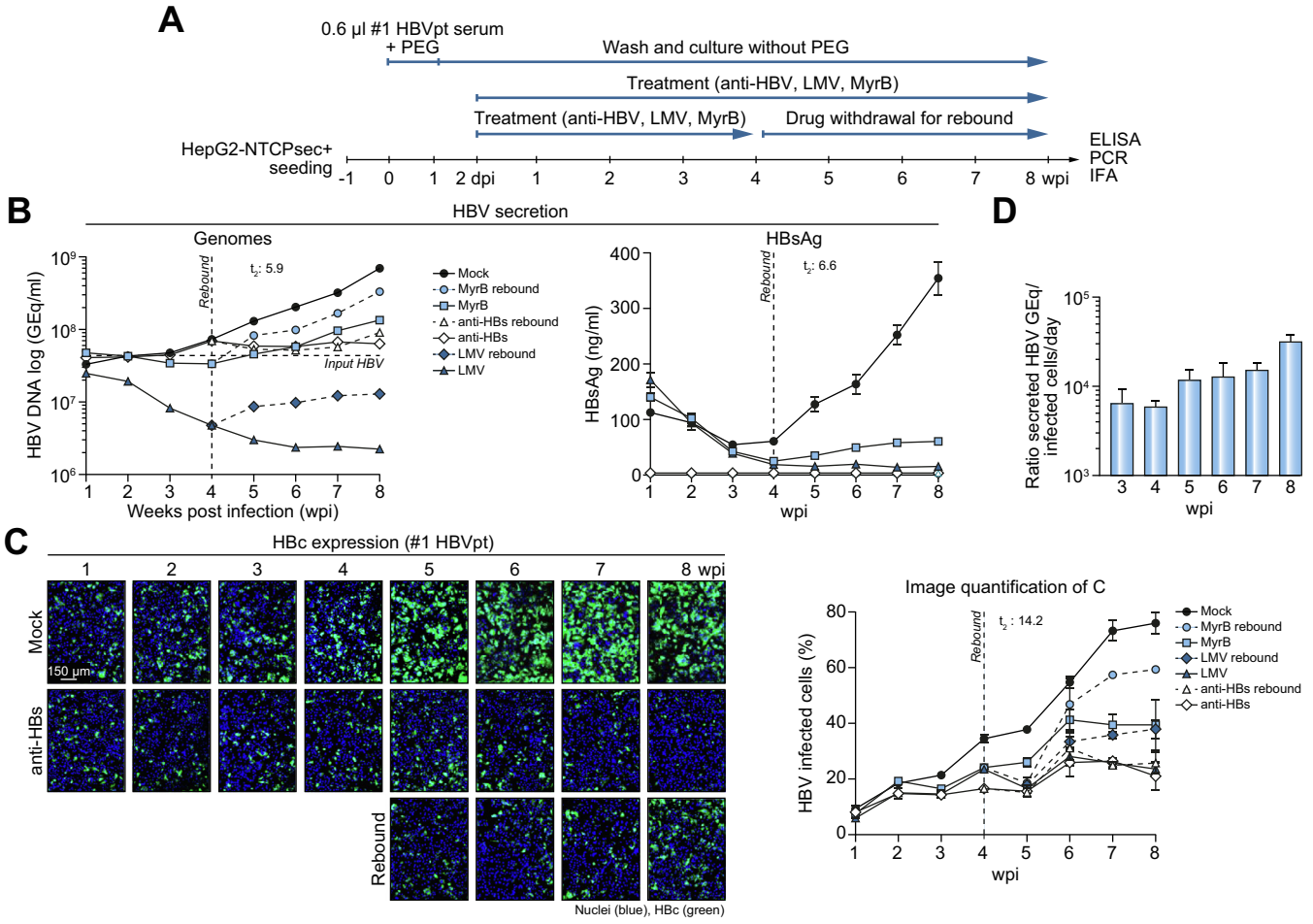

Fig. 7. Evaluation of inhibitors targeting amplification and spread of a HBV genotype C clinical sample in HepG2-NTCPsec+. (A) Workflow for 8-week long-term infection of HepG2-NTCPsec+ with HBVpt (#1) in the presence or absence of indicated inhibitors, as well as for inhibitor rebound experiments. (B) Concentrations of secreted HBV genomes and HBsAg. Horizontal line indicates inoculum concentration of HBV genomes (input). Supernatants of 8 wells (384-well plate) were pooled and analyzed as duplicates by ELISA and qPCR. (C) Representative images of mock- or anti-HBs-treated HBV-infected cells and of HBV-infected cells following of anti-HBs discontinuation. Quantification of infected cells in anti-HBs, LMV, or MyrB treatment and rebound experiments. (D) Calculations of secreted HBV genomes per infected cell per day. Vertical line indicates inhibitor discontinuation. Data presented as means ± SD of triplicate wells. (n.d., not detectable). HBeAg, HBV e antigen; HBs, HBV surface protein; HBV, hepatitis B virus; HBV; HBVpt, patient-derived HBV; LMV, lamivudine; MyrB, myrcludex B; RFP, red fluorescent protein; wpi, weeks post infection.

tocytes during an extended G1 phase and a prolonged cell cycle.[16] In HBV-transfected HepG2 cells, the formation of cccDNA and release of infectious viral progeny can be upregulated by G1 arrest.[17]

Furthermore, our results indicated that HBsAg envelopment and infectious HBV particle egress are cell-type-dependent. Supernatants of HBV-transfected HepAD38 cells harbored predominantly defective naked capsids, which were reported to exit stable HBV-transfected cells via an alternative secretion pathway compared to virions.[18] In contrast, infected HepG2-NTCPsec+ released high levels of LHBs-enveloped virions but no detectable naked capsids. An excess of secreted naked capsids is likely an aberrant product of transfected hepatoma cells where HBV replication is driven by chromosomally integrated HBV DNA, exhibiting epigenetic regulation distinct from that of viral replication driven by episomal cccDNA in infected cells. Naked capsids were also absent in the serum of patient #1. However, high levels of RNA-containing naked capsids were reported to be present in the blood of reverse transcription-inhibitor treated patients.[19] Whether the presence of naked capsids in the blood of some untreated patients is a product of an HBV secretion pathway or originates from damaged liver cells, remains controversial, as a recent study reported an association between circulating HBV RNA and serum alanine aminotransferase level.[20]

Considering the overall hepatocyte abundance in the liver and the low virus doses subjected to most common host-to-host transmission (*i.e.* sexual or percutaneous), infection begins with only a few infected cells and undetectably low viremia before the virus spreads through the liver within weeks or months, resulting in the establishment of acute HBV infection.[21] Restricted lifespans of cell cultures, generally not exceeding 3–4 weeks, have hampered *in vitro* investigations of late-phase kinetics of acute HBV infections. To mimic HBV amplification during acute infection establishment in the host, at least partially, we devised conditions for long-term infection experiments, including culturing of HepG2NTCPsec+ in 384-well plates with 2.5% DMSO and weekly medium exchanges. The 2 phases of viral amplification kinetics observed here may correlate with the so-called diagnostic window in patients with HBV: the virus is initially undetectable in the blood and increases exponentially during the subsequent viraemic ramp-up phase.

With a mean t_2 of 5.9 and 6.5 days for genotype C HBVpt and genotype D HBVcc, respectively, HepG2-NTCPsec+ amplified both viruses with nearly identical kinetics during the ramp-up phase (3–7 wpi). In contrast, the ramp-up phase in acutely infected patients exhibits an estimated t_2 of 2.2 to 5.8 days.[22] Inoculation of humanized uPA/SCID mice with higher viral loads accelerates the onset of the ramp-up phase to 1–2 wpi.[23] Here, the effect of viral dose on infection kinetics was confirmed, with high-titer inocula similarly promoting earlier onset of the viraemic ramp-up phase (1–2 wpi) in HepG2-NTCPsec+.

For 3 virus preparations, HBsAg and HBV DNA titer positively correlated in the supernatant of infected cells. However, relative to HepG2-NTCPsec+ infected with genotype B and D HBVcc, those infected with genotype C HBVpt produced more SHBs and LHBs-enveloped subviral particles per capsid (Fig. S9), but less HBV genomes, suggesting genotype-specific secretion patterns. In fact, the cells secrete 200- and 10-fold more genomes per SHBs when infected with genotype D HBVcc. Under the conditions tested, we observed max. 1,300- and 36,000-fold HBV genome and HBsAg amplification of genotype D HBVcc, respectively. With max. 50-fold, the genotype C HBVpt genome net amplification is significantly reduced which is due to the low infectivity of unpurified, crude patient serum as shown by the high minimum infectious dose of 2×10^7 GEq/ml needed for infection. Several factors may explain why our system is not as susceptible as shown for the chimpanzee model infected with inocula from patients in the pre-acute phase of infection.[24] Here, sera were collected from patients with CHB who are known to have a large proportion of non-infectious virus particles, *e.g.* antibody-neutralized virions, or preS1-rich filamentous subviral particles potentially competing with virions for the low-abundance preS1 receptor. Even the amplification potential for HBsAg cannot be calculated due to very high concentrations of subviral particles present in the serum of patients with CHB. However, the infection efficacy and net amplification may be further increased by purifying HBV, as preS1-containing subviral particles and virion-antibody complexes can be partially removed.

Mechanisms of HBV progeny amplification during the establishment of acute infection have remained poorly understood due to the lack of suitable cell culture models. However, we showed that the viraemic ramp-up phase was paralleled by *de novo* infection of naïve cells, indicating that viral spread contributed to amplification of HBV progeny. Spread was blocked by well described HBV entry inhibitors, reflecting interactions between viral surface proteins and cell membrane receptors (HSPGs and NTCP) as a restrictive step in HBV spread. Thus, spreading virions seem to utilize an identical entry mechanism to exogenously added virions during inoculation. However, more studies on HepG2-NTCPsec+ are needed to identify further cellular factors driving HBV spread.

In all HBV-susceptible cell culture models, efficient infection is strictly dependent on PEG during inoculation. PEG is required for the interaction of viral surface proteins with HSPG for HBV entry.[11] Recent reports have demonstrated that ~15% spread was achievable in a HepG2-NTCP cell line only under continuous PEG treatment.[25] However, HBV spread in HepG2-NTCPsec + from <10–80% infection rates in the absence of PEG, with PEG supplementation not affecting spread (Fig. S10B), indicating that progeny virions released by HepG2-NTCPsec+ can interact with HSPG for viral entry independently of PEG. We were unable to detect PEG-dependent- or independent spread in HepG2-NTCPsec− (Fig. S10C).

The high concentration of infectious HBV progeny in the supernatants would suggest spread via diffusion through an aqueous environment and random infection of single cells. However, spread was visualized as an expansion of HBV-infected cell clusters caused by a short-distance route of HBV spread to neighboring cells. Our model suggested that extracellular progeny virions released from *de novo* infected cells favored attachment to adjacent cells which required interaction with HSPG and NTCP at the plasma membrane for infection. In the chimeric uPA/SCID mouse HBV-infected clusters were not observed at 8 wpi, however, advanced microscopic studies on the spatial–temporal distribution of HBV-infected cells in the liver during acute infection establishment have not been conducted.[23]

During the viraemic ramp-up phase, intracellular cccDNA molecules and secreted virion rcDNA per infected cell increased simultaneously by 8- and 10-fold, respectively, corroborating that the cccDNA pool size is a critical factor for HBV amplification. Entry inhibitors prevented not only expansion of HBcAg-positive hepatocytes, but also the enhancement of the intrahepatic cccDNA pool and secreted progeny HBV, suggesting that cccDNA amplification is predominantly (88%) dependent on an extracellular route of receptor-mediated infection. This is in agreement with reports showing that MyrB blocks intrahepatic viral spread and cccDNA accumulation in humanized mice, with the authors concluding that intracellular recycling of nucleocapsids is only a minor route for cccDNA pool replenishment.[26] We estimated that, in HepG2-NTCPsec+, intracellular recycling of *de novo* synthesized nucleocapsids accounts for ≤12% of the cccDNA pool amplification.

Our cell culture platform combines 4 clinically relevant features of HBV-infected patients and animal models. First, HBV is efficiently amplified following *de novo* infection. Second, all released capsids are enveloped with LHBs and are highly infectious. Third, the observed kinetics of HBV amplification during the establishment of acute infection resemble the multiphasic kinetics observed in patients and infected chimeric uPA/SCID mice.[21–23] Fourth, like in infected chimpanzees, HBV does not induce any significant gene expression changes, underlining the reputation of HBV as a stealth virus.[15]

A hallmark of our HBV platform is the exceptionally efficient amplification and secretion of infectious viral progeny driven by episomal cccDNA which originates from *de novo* HBV entry. Compared to transfected hepatoma cells, HepG2-NTCPsec+ enable more physiological investigations of cccDNA epigenetic regulation and production of authentically enveloped, infectious HBV particles in concentrations suitable for analysis by electron microscopy. The platform can be further used for comparative characterizations of HBV variants, for the amplification of clinical isolates using minute amounts of crude HBV patient sera, and for the evaluation of HBV patient strain-specific features like infectivity, viability, replication efficiency and antiviral treatment sensitivity including neutralizing anti-HBV antibodies, viral rebound kinetics following inhibitor withdrawal and the evolution of drug-resistant mutant virus quasispecies under antiviral treatment pressure. Thus, this platform can elucidate the molecular biology underlying HBV morphogenesis, including envelopment, egress, secretion pathways and spread.

Financial support
This study was supported by the National Research Foundation of Korea (MSIT 2017M3A9G6068246 and NRF-2014R1A2A1A11052535) and the Gyeonggi Provincial Government.

Conflict of interest
The authors declare no conflicts of interest that pertain to this work.

Please refer to the accompanying ICMJE disclosure forms for further details.

Authors' contributions
A.K., J.Y., D.S. and M.P.W. designed experiments; A.K., J.Y., E.J., T. T.T., K.P., S.P., H.K. X.S., X.Q. X.H. performed experiments; J.Y.P., S.H.A., K.H.H., S.K.Y., J.H.K., W.S.R. provided significant resources. All authors contributed to the data analysis and interpretation, and A.K., W.H.G and M.P.W. wrote the manuscript.

Acknowledgements
We would like to thank Dieter Glebe (Giessen University) for providing antibodies and plasmids, and Gil-Je Lee and Ernest Jonathan Cechetto (Perkin-Elmer) for technical assistance in handling microscopy samples and for providing support for the phenotypic analysis of HBV cluster formation. We would like to thank Eunjin Do (Yonsei University) for technical assistance in cccDNA Southern blotting, Stephan Urban and Yi Ni (Heidelberg University) for providing protocols and technical support for the isolation of infectious virions from HepAD38 cells, and Inyoung Kim (Blickfang designstudio) for graphic design support. We thank Heinz. We thank the National Research Foundation of Korea (MSIT and NRF) and the Gyeonggi Provincial Government for financial support.

Supplementary data
Supplementary data to this article can be found online at https://doi.org/10.1016/j.jhep.2019.04.010.

References
Author names in bold designate shared co-first authorship

[1] World Health Organization. Hepatitis B: fact sheet. World Heal Organ 2017.
[2] Lempp FA, Wiedtke E, Qu B, Roques P, Chemin I, Vondran FWR, et al. Sodium taurocholate cotransporting polypeptide is the limiting host factor of hepatitis B virusinfection in macaque and pig hepatocytes. Hepatology 2017:703–716.
[3] Burwitz BJ, Wettengel JM, Mück-Häusl MA, Ringelhan M, Ko C, Festag MM, et al. Hepatocytic expression of human sodium-taurocholate cotransportingpolypeptide enables hepatitis B virus infection of macaques. Nat Commun 2017:2146.
[4] **König A**, **Döring B**, Mohr C, Geipel A, Geyer J, Glebe D. Kinetics of the bile acid transporter and hepatitis B virus receptor Na+/taurocholate cotransporting polypeptide (NTCP) in hepatocytes. J Hepatol 2014;61:867–875.
[5] Gripon P, Rumin S, Urban S, Le Seyec J, Glaise D, Cannie I, et al. Infection of a human hepatoma cell line by hepatitis B virus. Proc Natl Acad Sci U S A 2002;99:15655–15660.
[6] Winer BY, Huang TS, Pludwinski E, Heller B, Wojcik F, Lipkowitz GE, et al. Long-term hepatitis B infection in a scalable hepatic co-culture system. Nat Commun 2017:125.
[7] Ortega-Prieto AM, Skelton JK, Wai SN, Large E, Lussignol M, Vizcay-Barrena G, et al. 3D microfluidic liver cultures as a physiological preclinical tool for hepatitis Bvirus infection. Nat Commun 2018:682.
[8] Shlomai A, Schwartz RE, Ramanan V, Bhatta A, de Jong YP, Bhatia SN, et al. Modeling host interactions with hepatitis B virus using primary and induced pluripotent stem cell-derived hepatocellular systems. Proc Natl Acad Sci U S A 2014;111:12193–12198.
[9] Xia Y, Carpentier A, Cheng X, Block PD, Zhao Y, Zhang Z, et al. Human stem cell-derived hepatocytes as a model for hepatitis B virus infection, spreading and virus-host interactions. J Hepatol 2017;66:494–503.
[10] Yan H, Zhong G, Xu G, He W, Jing Z, Gao Z, et al. Sodium taurocholate cotransporting polypeptide is a functional receptor for human hepatitis B and D virus. Elife 2012;2012.
[11] Schulze A, Gripon P, Urban S. Hepatitis B virus infection initiates with a large surface protein-dependent binding to heparan sulfate proteoglycans. Hepatology 2007;46:1759–1768.
[12] Hu J, Lin YY, Chen PJ, Watashi K, Wakita T. Cell and Animal Models for Studying Hepatitis B Virus Infection and Drug Development. Gastroenterology 2019:338–354.
[13] Ko C, Park WJ, Kim S, Windisch MP, Ryu WS, et al. The FDA approved drug irbesartan inhibits HBV-infection in HepG2 cells stably expressing sodium taurocholate co-transporting polypeptide. Antivir Ther 2015;20:835–842.
[14] Ni Y, Lempp FA, Mehrle S, Nkongolo S, Kaufman C, Fälth M, et al. Hepatitis B and D viruses exploit sodium taurocholate co-transporting-polypeptide for species-specific entry into hepatocytes. Gastroenterology 2014:1070–1083.
[15] Wieland S, Thimme R, Purcell RH, Chisari FV. Genomic analysis of the host response to hepatitis B virus infection. Proc Natl Acad Sci U S A 2004;101:6669–6674.
[16] Quasdorff M, Hösel M, Odenthal M, Zedler U, Bohne F, Gripon P, et al. A concerted action of HNF4alpha and HNF1alpha links hepatitis B virus replication to hepatocyte differentiation. Cell Microbiol 2008.
[17] Zhang X, Zhang E, Ma Z, Pei R, Jiang M, Schlaak JF, et al. Modulation of hepatitis B virus replication and hepatocyte differentiation by MicroRNA-1. Hepatology 2011.
[18] Zeyen L, Prange R. Host Cell Rab GTPases in Hepatitis B Virus Infection. Front Cell Dev Biol 2018:154.
[19] Bai L, Zhang X, Kozlowski M, Li W, Wu M, Liu J, et al. Extracellular hepatitis B virus RNAs are heterogeneous in length and circulateas capsid-antibody complexes in addition to virions in chronic hepatitis b patients. J Virol 2018;92, pii: e00798-18.
[20] **van Campenhout MJH**, **van Bömmel F**, Pfefferkorn M, Fischer J, Deichsel D, Boonstra A, et al. Host and viral factors associated with serum hepatitis B virus RNA levels among patients in need for treatment. Hepatology 2018:839–847.
[21] Barker LF, Murray R. Relationship of virus dose to incubation time of clinical hepatitis and time of appearance of hepatitis-associated antigen. Am J Med Sci 1972;263:27–33.
[22] Whalley SA, Murray JM, Brown D, Webster GJ, Emery VC, Dusheiko GM, et al. Kinetics of acute hepatitis B virus infection in humans. J Exp Med 2001.
[23] **Ishida Y**, **Chung TL**, Imamura M, Hiraga N, Sen S, Yokomichi H, et al. Acute hepatitis B virus infection in humanized chimeric mice has multiphasic viral kinetics. Hepatology 2018;00:1–12.
[24] Komiya Y, Katayama K, Yugi H, Mizui M, Matsukura H, Tomoguri T, et al. Minimum infectious dose of hepatitis B virus in chimpanzees and difference in the dynamics of viremia between genotype A and genotype C. Transfusion 2008;48:286–294.
[25] Michailidis E, Pabon J, Xiang K, Park P, Ramanan V, Hoffmann H-H, et al. A robust cell culture system supporting the complete life cycle of hepatitis B virus. Sci Rep 2017;7:16616.
[26] **Volz T**, **Allweiss L**, ḾBarek M Ben, Warlich M, Lohse AW, Pollok JM, et al. The entry inhibitor Myrcludex-B efficiently blocks intrahepatic virus spreading in humanized mice previously infected with hepatitis B virus. J Hepatol 2013;58:861–867.